PRELIMINARY STUDIES FOR USING MAGNETIC RESONANCE IMAGING SYSTEMS AS A MEAN OF PROPULSION FOR MICROROBOTS IN BLOOD VESSELS AND EVALUATION OF FERROMAGNETIC ARTEFACTS

Jean-Baptiste Mathieu[1], Sylvain Martel[1], L'Hocine Yahia[2],
Gilles Soulez[3], Gilles Beaudoin[3]

[1]NanoRobotics Laboratory, École Polytechnique de Montréal, Canada
[2]Biomechanics/Biomaterials Research Group, Department of Mechanical Engineering, École Polytechnique de Montréal, Canada
[3]Radiology Department, Faculty of Medicine, Université de Montréal, Canada
e-mail : jean-baptiste.mathieu@polymtl.ca

Abstract

A prototype for a magnetically controlled microrobot for applications in blood vessels is being developed. A strong and variable driving magnetic field exerts propulsion forces in three dimensions to a ferromagnetic core embedded onto the microrobot. Magnetic Resonance Imaging (MRI) systems are being considered as they provide the required magnetic fields and controls. Their imaging capabilities could also be used to track the displacements of the robots, providing position feedback informations. The paper describes tests made for spin echo and gradient echo sequences. They show that ferromagnetic materials cause imaging distortions (artefacts) several times larger than the size of the ferromagnetic core. It is critical to retrieve the robot's position from the distorted image but, the elimination or reduction of such ferromagnetic artefacts is currently a serious problem. Therefore, alternative solutions to the imaging problems like artefact cancelation or artefact pattern tracking softwares need to be developed.

Keywords: magnetic resonance imaging, microrobot, blood vessels.

1. INTRODUCTION

Medical applications of microrobots driven inside the blood vessels are numerous. Some are Minimally Invasive Surgeries (MIS) like angioplasties, highly localized drug deliveries for chemotherapy or biopsies. The smaller these robots are, the wider the operating range becomes through accesses to the finest blood vessels such as capillaries. Such system could potentially be released in the vicinity of the treatment area through a catheter. Then, it could be externally guided using a control software able to track it, compute its trajectory and then determine the magnetic field gradient to be applied on it. This magnetic propulsion concept is extremely promising for miniaturized systems targetted at in vivo applications.

The quantity of ferromagnetic particles needed, which is related to the size of the robot, is determined by the blood flow at the location where the treatment is to be performed within the body. Such a propulsion system can be easily made larger or smaller accordingly to the robot's task and location within the body. This is not the case for internal propulsion systems previously proposed in the literature such as micromotors that involve complex and precise assembly of numerous moving parts with the additional need to carry along their energy source, a major bottleneck in miniaturization. To achieve further miniaturization within the body, Magnetic Resonance Imaging (MRI) systems were chosen as the mean of propulsion for the proposed microrobot. The main advantages of this approach is that our previous studies show that MRI systems provide adequate magnetic field and gradients for propulsion and they are already present in almost every hospital. As such, the microrobot is referred to as MR-Sub: Magnetic Resonance-Sub. This paper describes the results of our preliminary MRI tests that aimed the evaluation of the imaging distortions induced by the presence of ferromagnetic materials in a MRI system.

0-7803-7781-8/03/$17.00

2. BACKGROUND

Because of its larger diameter, the arterial system is being considered as the initial target location where the microrobot will be implanted. Later, with further miniaturization and more precise imaging techniques, smaller regions such as capilllaries could also be considered. The dimensions of the blood vessels in human typically range from 25 mm in diameter (aorta) to approximately 8 μm (capillaries) [1]. The blood flow in the arterial system is pulsatile and much faster at the exit of the heart (ascending aorta: maximal systolic velocity is 1120 mm/s) [2]. When an artery or vein bifurcates, the cross-sectional area of its branches exceeds that of the parent vessel. Therefore, the blood velocity decreases away from the heart in a similar fashion when water in a rushing stream slows down when entering a broad pool [1].

The magnetic force induced by the MRI system must be stronger than the drag force of the blood flow on the microrobot for motion to take place and to allow control in displacement. The torque and the force induced by an MRI system can be estimated [3] from

$$\vec{\tau} = \vec{m} \times \vec{B} = \vec{M} * V_{ferro} \times \vec{B} \quad (1)$$

$$\vec{F}_{\text{magnetic}} = \vec{M} . V_{ferro} . \nabla \vec{B} \quad (2)$$

In Eqs. 1 and 2, τ is the magnetic torque (N.m), $\vec{F}_{\text{magnetic}}$ is the magnetic force (N), $\vec{M}$ is the magnetization of the material (A/m), V_{ferra} is the volume of the ferromagnetic body (m^3), $\vec{B}$ is the magnetic induction (T) and $\nabla \vec{B}$ is the gradient (spatial variation) of the magnetic induction (T/m).

3. MATERIALS AND METHODS

A first series of MRI tests was conducted. As stated previously, the goal of the experiment was to observe the effect of ferromagnetic bodies on the images created by an MRI system. A list of the various ferromagnetic samples used for the experiments is depicted in Table 1.

Table 1. Ferromagnetic samples imaged

Sample Number	Description
1	440-C Stainless Steel Precision Ball, 1/16" Dia., Grade 24
2	Cobalt Steel Round Blanks, 1/64" Dia., 1-1/2" Length
3	Chrome Steel Ball, 1/16" Dia., Grade 25
4	1010/1020 Carbon Steel Ball, 1/8" Dia., Grade 1000
5	440-C Stainless Steel Ball, 1/16" Dia., Grade 100

All tests were performed on a 1.5-T Siemens Magnetom Vision system.

In order to be able to measure an MRI signal, ferromagnetic bodies have to be immersed in an aqueous medium. As such, the ferromagnetic samples were placed inside small oranges with a diameter of approximately 50 mm. Oranges contain water and their well-known structure allows easy recognition of signal and geometric artefacts. Five oranges were incised. One ball of each composition (samples 1, 3, 4, 5 in Table 1) as well as the cobalt steel bar (sample 2) were buried inside a separate orange. In a first imaging set-up, all five oranges were placed inside the MRI system in the manner shown in Fig. 1.

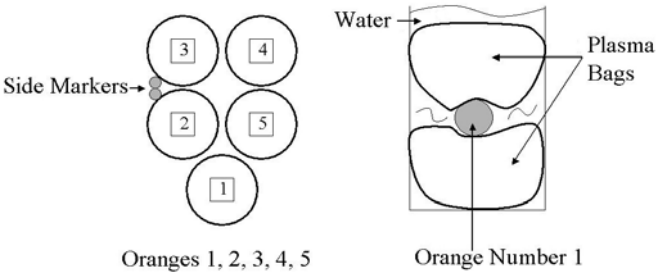

Fig. 1. First (left) and second (right) experimental set-ups

Oranges were numbered according to the sample they contained. Two side markers were added to differentiate oranges 2 and 3 from oranges 4 and 5. The first goal of this set-up was to get an order of magnitude of the artefacts size and to observe their geometry. It also allowed us to compare the artefacts of the different samples. It was used for imaging series A.

A second set-up was also used to obtain a better view of one single artefact in its full extent. Orange number 1 was immersed inside of a water tank. It was placed between two plasma bags full of water that prevented it from moving while imaging. This set-up offered a better view of one single artefact and an aqueous volume large enough to contain it completely. It was used for series B and C.

For the localization of the ferromagnetic bodies with the first and the second set-ups, fast gradient echo scans of the imaging volume were used. Sequence parameters were TR: 450 ms and TE: 12 ms with the resulted echo gradient images with set-up 2 shown in Fig. 2.

For the imaging series A, spin echo images were taken in the coronal plane. Slices thickness was 3 mm, distance between slices was 1.5 mm and phase encoding was left-right. The presence of the five ferromagnetic bodies prevented the shim routine of the main magnetic field to converge. This is shown in Fig. 3.

The imaging series B and C were done using spin echo sequences with a 3 mm slice thickness and a 3 mm distance between slices. Series B and C were made in the sagittal

plane and phase encoding was anterior posterior for B and head-feet for C. As only one ball was present inside of the magnetic field, the shim routine was able to converge. This is shown in Fig. 4 and Fig. 5.

4. RESULTS

As shown in Fig. 2, the effect of ferromagnetic presence on gradient echo images are geometric distortions as well as signal losses.

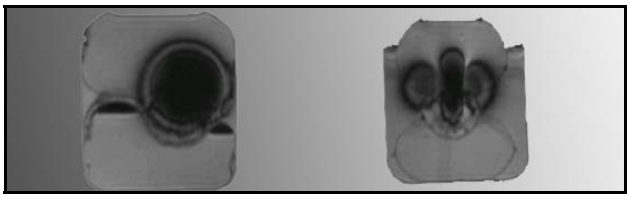

Fig. 2. Echo gradient images for the second set-up

Spin echo sequences are less sensitive to magnetic field distortions that ferromagnetic bodies might induce [4]. However, the images acquired (Fig. 3, 4 and 5) using a spin echo sequence are long to generate. It took approximately 5 minutes to scan the volume containing the five oranges. Serious geometrical distortions as well as zones with low signals or saturated signals were observed. "The characteristic appearance of the image is a low-intensity region or signal void adjacent to or surrounded by regions of high intensity. Very often, bizarre, non-anatomic, elongated distortions are seen. Depending on the quantity, shape, and susceptibility of the metal present, there may be so much distortions that the image is anatomically unrecognizable"[5].

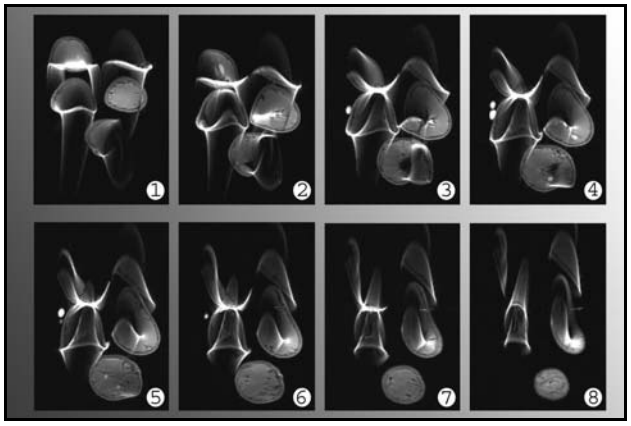

Fig. 3. Images of series A with slice numbers

The volume of the artefacts that were generated was larger than we first predicted. They could not be imaged completely because they stretched outside of the oranges where there was no more water. The artefacts of the different ferromagnetic bodies overlapped each other. It was impossible to observe them separately because every ferromagnetic body had an effect on the others. This size problem makes the localization of the ferromagnetic bodies in the image more difficult.

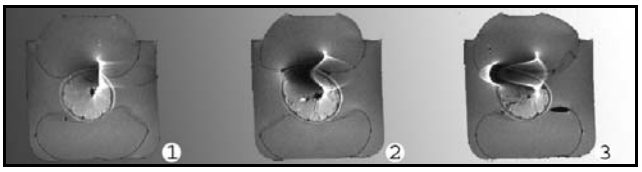

Fig. 4. Images of series B with slice numbers

The second set-up allowed us to observe the same kind of artefacts as the first one, but provides a much better view of it. While generating an MRI image, lines and columns can be encoded using either phase or frequency. If lines are encoded using the phase, columns will be encoded using frequency and conversely.

In imaging series C, the artefact tilted with a 90° angle compared to series B (Fig.4 and 5). It remained oriented along the frequency encoding direction. This information confirms the results obtained by Hendrick [5].

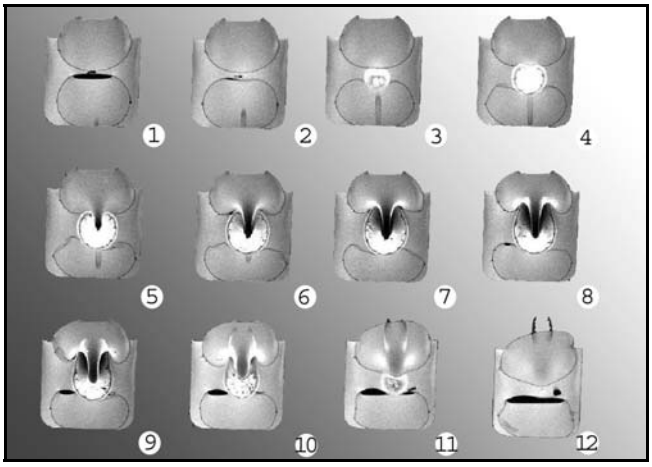

Fig. 5. Images of series C with slice numbers

5. DISCUSSION

These tests aimed at getting a first concrete idea of the imaging problems that will have to be solved in order to control the MR-Sub. There is no direct method of tracking the MR-Sub because of the tremendous three-dimensional complexity and important size of the artefacts. "Ferromagnetic objects produce artefacts because of their higher magnetic susceptibility relative to tissue, which produces localized magnetic field inhomogeneities. This

results in image distortion and associated contrast changes" [5].

Moreover, the artefacts depend on the MRI sequence that is used.

In an MRI system, supra-conductive coils generate a magnetic field H_o (A/m) in space. This magnetic field induces the magnetic induction B_o (T) according to

$$\vec{B}_0 = \mu_0 . \vec{H}_0 \quad (3)$$

In Eq. 3, μ_o is the vacuum magnetic permeability ($4.\pi.10^{-7}$ H/m). When it is applied on a ferromagnetic body, the magnetic field H_o (A/m) induces a magnetization M (A/M) in it. The combined action of H_o and M distorts B_o (Eq. 4).

$$\vec{B}_0 = \mu_0 . (\vec{H}_0 + \vec{M}) \quad (4)$$

MRI images are generated according to Eq. 3, hence they do not take the presence and effect of a ferromagnetic body into account. This presence modifies the Larmor frequency and the relaxation parameters of the hydrogen atoms surrounding the ferromagnetic body [7] as well as the positioning gradients [5]. This gives rise to imaging distortions in the intensity and in the position assigned to each pixel in the image.

One of the causes of signal distortions can be the modification of the slice selection gradient. If the ferromagnetic body makes the slice selection gradient steeper, the signal gets lower. The reason is that the spatial zone where the atoms have the proper Larmor frequency becomes thinner. If the ferromagnetic body makes the gradient less pronounced, the MRI signal gets stronger because the slice becomes thicker and more atoms respond to the Radio Frequency (RF) excitation [5]. Distortions in the signal intensity can be caused also by the modification of the relaxation parameters of the atoms.

One cause of the geometric distortions can be the effect of the magnetization M on the phase and frequency encoding gradients. An MRI system assigns the appropriate value to a pixel because the phase and frequency gradients are used to encode the line and column in which a given atom belongs in the signal it emits [7]. The ferromagnetic body can also modify the frequency and phase of the MR signals. As the image generated does not take these modifications into account, it may assign a wrong position on the monitor to some elements of the scanned volume because of the presence of the ferromagnetic body. A ferromagnetic body induces around itself complex three-dimensional distortions of the main magnetic field and of its gradients. The effect of these distortions on the image is even more complex since they affect several steps of the imaging process. Therefore, the link between the cause (ferromagnetic body) and the effect (image distorted in intensity and geometry) is far from being straightforward.

6. CONCLUSION

An important goal of the MR-Sub project is the control of a robot using a MRI magnetic field. Therefore, it is critical to retrieve the position of the robot from the distorted images. An image processing study must be done in order to bypass the obstacles due to ferromagnetic artefacts. There are two initial approaches that may be investigated. The first one would cancel the artefacts by modifying the MRI machine and its software in order to take into account the presence of the ferromagnetic body during the image generation. A mathematical model of MR-Sub's magnetization has to be performed. The modified MRI-based software would then compensate its effects on every step of the imaging process. Another approach would be to develop an image-processing algorithm to track a known artefact in the distorted image from its mathematical model or from an artefact database. Once the artefact is found, it would be linked to the robot's position. The control of MR-Sub would then be potentially feasible.

Acknowledgements

This work is supported in part by the Canada Research Chair (CRC) in Conception, Fabrication, and Validation of Micro/Nanosystems and by the Natural Sciences and Engineering Research Council of Canada (NSERC).

References

[1] R.F. Rushmer, *STRUCTURE AND FUNCTION OF THE CARDIOVASCULAR SYSTEM.* W. B. Saunders Company, 1972

[2] W.R. Milnor, *HEMODYNAMICS.* Williams & Wilkins, 1982

[3] W.F. Brown, *PRINCIPES DE FERROMAGNÉTISME*. Monographies Dunod, 1970

[4] B. Kastler, *PRINCIPES DE L'IRM, MANUEL D'AUTO APPRENTISSAGE*. Collection d'imagerie radiologique, Masson, 1994

[5] R. E. Hendrick, P. D. Russ, J. H. Simon, *MRI: PRINCIPLES AND ARTIFACTS*. Raven Press, 1993

[6] D. Jiles, *INTRODUCTION TO MAGNETISM AND MAGNETIC MATERIALS*. Chapman and Hall, 1990

[7] B. Kastler, *COMPRENDRE L'IRM : MANUEL D'AUTO-APPRENTISSAGE*. Collection d'imagerie radiologique, 3'rd Ed., 2000